Materials and Design 108 (2016) 470–478

Contents lists available at ScienceDirect

Materials and Design

journal homepage: www.elsevier.com/locate/matdes

High volume-fraction silk fabric reinforcements can improve the key mechanical properties of epoxy resin composites

Kang Yang [a,b], Robert O. Ritchie [b,c], Yizhuo Gu [a], Su Jun Wu [a,b], Juan Guan [a,b,d,*]

[a] School of Materials Science and Engineering, Beihang University, Beijing 100191, China
[b] Intl. Research Centre for Advanced Structural and Biomaterials, Beihang University, Beijing 100191, China
[c] Department of Materials Science & Engineering, University of California, Berkeley, CA 94720, USA
[d] State Key Laboratory of Molecular Engineering of Polymers, Fudan University, Shanghai 200433, China

HIGHLIGHTS

- Environmentally friendly silk fibres were used to reinforce a widely used commercial epoxy resin.
- The effect of volume fraction of the reinforcement silk on the mechanical properties of the composite was studied.
- A highest volume fraction of the silk reinforcement in this work was 70 vol.%.

GRAPHICAL ABSTRACT

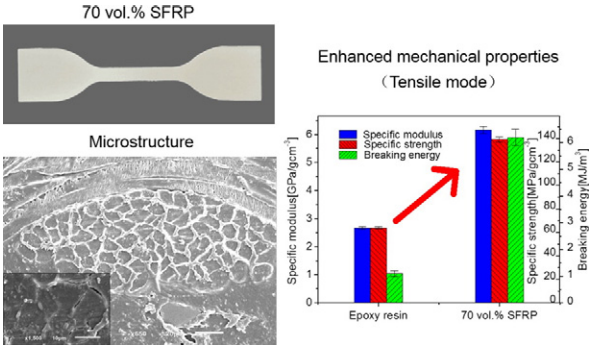

ARTICLE INFO

Article history:
Received 8 June 2016
Received in revised form 28 June 2016
Accepted 29 June 2016
Available online 1 July 2016

Keywords:
Fibre composite
Thermosets
Glass transition
Dynamic mechanical thermal analysis
Structure-property relations
Impact resistance

ABSTRACT

Silk fabric reinforced epoxy composites (SFRPs) were prepared by simple hot-press and vacuum treatment, to achieve a maximum reinforcement fraction of 70 vol.%-silk. Mechanical behaviour, specifically tensile, flexural, interlaminar shear, impact, dynamic and thermal properties of the SFRPs, was investigated. It was shown that reinforcement by silk fabric can greatly enhance the mechanical performance of SFRPs. In particular, the tensile modulus and breaking energy of 70 vol.%-silk SFRP were 145% and 467% higher than the pristine epoxy resin. Moreover, the flexural modulus, ultimate strength and breaking energy were also markedly increased for SFRPs. The flexural strength increased linearly with increasing silk volume fraction from 30 to 60 vol.% but diminished slightly at 70 vol.%. Additionally, interlaminar shear results showed that the silk and the matrix epoxy resin had better adhesion properties than plain woven flax fibre. Of most significance is that the impact strength reached a maximum of ~71 kJ m^{-2} for the 60 vol.%-silk SFRP, which demonstrates the potential of silk reinforcements in impact-resistant composites for applications such as wind turbine blades. Our study may shed light on improving the strength and toughness of engineering composites by incorporating high volume fractions of natural fibres.

1. Introduction

Natural fibre reinforced composites have recently been the subject of extensive research [1–3], propelled firstly by their potential

* Corresponding author at: School of Materials Science and Engineering, Beihang University, Beijing 100191, China.
E-mail address: juan.guan@buaa.edu.cn (J. Guan).

http://dx.doi.org/10.1016/j.matdes.2016.06.128
0264-1275/

applications due to their low density, high specific mechanical properties and promising biodegradability and secondly by the environmental and social demands for a sustainable world. Silk fibre reinforced epoxy materials embody one such class of composites. In this regard, compared with the flax-represented plant fibres, the best-known fashion silk from silkworm *Bombyx mori* (*B. mori*) represents the only natural fibre which can be used as a continuous filament of fibrous protein. Despite this, silk reeled from cocoons and fed to the textile industry in the silk commercial value chain is rarely utilized for practical engineering. However, this strong and tough protein fibre may endow modern engineering composites with unprecedented mechanical properties, as has been suggested in several recent studies on silk-composites [1,3].

Shah et al. [4], for example, prepared nonwoven (from natural cocoon walls) and woven (from silk fabric) silk fibre reinforced plastics (SFRPs) via vacuum-driven resin transfer moulding. The fibre volume fraction and density of the SFRPs were, respectively, 36.2% and 1.20 g cm^{-3} for the nonwoven and 45.2% and 1.22 g cm^{-3} for the biaxial-woven. These SFRPs displayed much greater tensile and flexural specific strengths (~90 MPa/g cm^{-3} and ~13 $MPa^{1/2}$/g cm^{-3}), impact strength (115 kJ m^{-2}) and inter-laminar shear strength (~92 kJ m^{-2}/g cm^{-3}) than those of flax fibre reinforced epoxy resin plastics; indeed, they are comparable, although not necessarily superior, to those of glass fibre reinforced epoxy resin composites. In particular, the plain woven SFRPs demonstrated the high ductility (e.g., tensile fracture strain of 7%) of silk-fibre composites.

With respect to biodegradable-polymer based silk composites, Ho et al. [5] manufactured a silk fibre reinforced biodegradable plastic poly(lactic acid) (PLA) with 5 wt.% silk by small scale injection moulding; this material had tensile and flexural moduli that were, respectively, 27% and 2% higher than pure PLA. Similarly, Zhao et al. [6] showed with as little as 5 wt.% incorporation of silk the dynamic mechanical, thermal and biodegradable properties of silk/PLA biocomposites could be improved markedly. Shubhra et al. [7] studied the mechanical and degradation characteristic of silk fibre reinforced gelatine composites, and measured tensile strengths, tensile modulus, bending strengths, bending modulus and impact strengths that were, respectively, ~260%, 400%, 320%, 450% and 260% higher than the unreinforced matrix material. A series of novel silk fibroin fibre/poly(ε-caprolactone) (PCL) biocomposites with different silk contents, prepared by Li et al. [8] showed the highest strength with 35 to 45 wt.% silk contents; the 35% silk composite had the highest tensile strength whereas the 45% silk composite showed the best flexural strength. These results provide evidence of the important role of silk fibres as a reinforcement phase to improve the mechanical properties of PCL. In similar vein, an all-silk composite made of silk fibre embedded in a reconstituted silk fibroin matrix with various weight fractions of silk fibre, prepared by Yuan et al. [9], showed the best tensile strength (151 ± 5 MPa) and breaking strain (27.1 ± 1.4%) with 25 wt.% silk fibre reinforcement.

The properties including physical, tensile mechanical and flexural mechanical properties, from the abovementioned references are consolidated and compared with those of typical flax fibre reinforced epoxy resin (thermosets) and glass fibre reinforced epoxy resin (thermosets) in Table 1.

Shah et al. [1] also examined the through-thickness compaction behaviour of three fibre reinforcements, namely, silk, plant fibre and glass fibre, and under the same compaction pressure biaxial silk fabric was more compressible than flax plant fibre and glass fibre. This indicates that silk fabric can reinforce fibre composites that require higher volume fractions, a problem which until now has been a "show stopper" for plant fibre reinforcements.

Of all the thermosetting resins, epoxy resin is one of the most widely used owing to its many credentials such as easy processibility, low cost, reasonable mechanical properties, good adhesive performance, good chemical resistance and great high-temperature tolerance [10–13]. Epoxy resin-based composites have been used extensively in electronics, aerospace and civil engineering [14–17]. However, due to the high degree of cross-linking, many products of epoxy resin are intrinsically very brittle, and the impact strength is low (shown as a catastrophic failure). This weakness in the mechanical performance has compromised the use of epoxy resin for many structural applications. As a result, modifications of the epoxy resin products for enhanced mechanical properties, especially impact strength and toughness, have become an important area for research [18–20], with the use of natural fibre reinforcements to improve their mechanical performance proving a popular approach [21–24].

Table 1
Summary of the properties of the silk fibre reinforced composites (SFRPs), as compared to flax fibre reinforced epoxy resin composites (FFRPs) and glass fibre reinforced epoxy resin composites (GFRPs). Interlaminar shear strength is shortened as ILSS in the unit of MPa.

Composite	Physical properties		Tensile mechanical properties			Flexural mechanical properties			ILSS (MPa)	Impact strength ($kJ \cdot m^{-2}$)
	Fibre volume fraction (%)	Density ($g \cdot cm^{-3}$)	Stiffness (GPa)	Ultimate strength (MPa)	Ultimate strain (%)	Stiffness (GPa)	Ultimate strength (MPa)	Ultimate strain (%)		
Nonwoven silk–epoxy [4]	36.2	1.20	5.4 ± 0.2	60 ± 5	1.3 ± 0.1	5.2 ± 0.2	143 ± 10	3.4 ± 0.4	31.0 ± 3.7	16 ± 1
Plain woven silk–epoxy [4]	45.2	1.22	6.5 ± 0.1	111 ± 2	5.2 ± 0.2	6.4 ± 0.4	250 ± 4	6.9 ± 0.2	42.6 ± 5.9	115 ± 7
Nonwoven flax–epoxy [4,22]	15–35	1.20–1.26	5.8–9.8	37–75	0.8–1.6	4.8–6.7	55–91	2.1–3.2	13.6–26.7	8–15
Plain woven flax–epoxy [4,22]	30–55	1.24–1.32	7.3–11.2	63–89	1.5–2.9	2.1–10.1	57–195	3.3–4.9	9.7–23.3	23–36
Nonwoven glass–epoxy [4,22]	15–45	1.36–1.80	10.2–16.7	123–241	1.0–2.1	9.0–11.4	192–325	3.0–4.0	25.0–35.0	73–107
Plain woven glass–epoxy [4,22]	30–65	1.58–2.09	17.0–24.0	350–500	2.1–2.5	13.2–22.0	370–560	3.5–4.0	38.0–52.0	165–280
Silk-PLA [5]	5	–	4.08 ± 0.05	70.6 ± 1.1	3.8 ± 0.5	4.06 ± 0.2	97.4 ± 21.8	2.9 ± 0.9	–	–
10% silk fibre/fibroin [9]	10	–	3.1 ± 0.2	83 ± 7	11.2 ± 1.3	–	–	–	–	–
20% silk fibre/fibroin [9]	20	–	3.0 ± 0.2	142 ± 7	23.5 ± 17	–	–	–	–	–
25% silk fibre/fibroin [9]	25	–	2.8 ± 0.1	151 ± 5	27.1 ± 1.4	–	–	–	–	–
Silk fibre/gelatin [7]	20	–	0.65	44.5	8.2	3.7	63	–	–	5.1
Silk fibre/PCL [8]	35	–	–	26.5	12.0	1.8	49	–	–	–
Silk fibre/PCL [8]	45	–	–	22.5	5.0	2.1	59.5	–	–	–

The aim of this work was to further evaluate the processing and properties of silk fibre reinforced epoxy resin composites with high fibre volume fractions, with the objective of enhancing the mechanical properties of pristine epoxy resin. The high-volume fibre fraction was achieved by adopting a widely used and easily accessible thermoset manufacturing method, that of the hot-press moulding. This processing technology is considered to be an improvement over the one used in Shah et al.'s [4] study, which employed vacuum-driven resin transfer moulding, as higher fibre volume-fraction can be achieved by applying higher pressures (>100 kPa). The mechanical properties of these composites were comprehensively evaluated, specifically the tensile, flexural, interlaminar shear and impact properties, together with dynamic mechanical thermal analysis to investigate the thermo-mechanical changes in the composites, particularly in glass-transition region. Our results demonstrate that silk fabrics can significantly improve the mechanical behaviour and impact properties of brittle epoxy resin thermosets, which could open new opportunities for the applications of these interesting polymeric materials.

2. Materials and methods

2.1. Materials

Epoxy resin E-51 with curing agent DS-300G, supplied by Dasen Material Science & Technology. Inc. (Tianjin, China), was used as the thermoset epoxy matrix material. Epoxy resin E51 is bisphenol A type of epoxy and the formula is shown below. The viscosity was measured to be ~40 mPa s. The hardener used modified aromatic amine curing agent. The curing reaction was between epoxy groups in E51 and amine groups in the curing agent. The mass ratio of E-51 and DS-300G was 1:0.84.

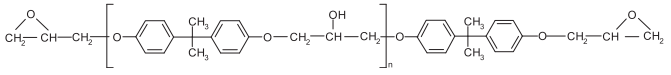

According to the manufacturing company, the E-51 resin product has a cured density ρ_e of 1.20 g cm^{-3}. The tensile modulus E_t, strength σ_t and ultimate strain ε_t were, respectively, 3.0–3.2 GPa, 73–78 MPa and 2.7–2.9%, with an impact strength of 12.5–13.0 kJ m^{-2}.

A plain woven fabric (areal density of 90 ± 5 g m^{-2}), supplied by Huzhou Yongrui Textile Co. Ltd. (Zhejiang Province, China), was used as the silk fibre reinforcement. The fibre yarn contained about 80 threads of silk on each direction. The density of the silk fabric ρ_f was assumed to be 1.3 g cm^{-3} [25].

2.2. Fabrication of composites

Composite laminates were fabricated by hand lay-up followed by hot pressing. Depending on the target volume fraction of the silk fabric, silk fabrics of size 200 × 100 mm were carefully brushed with different amounts of uncured epoxy resin and laid up in an open mould. In the hot-press process, specimens were cured at an isothermal temperature of 120 °C for 2 h with a compaction pressure of 300 kPa. Silk fabric reinforced composites with a dozen different volume fractions (v_f) from 30% to 70% were prepared, and SFRPs with 29.33%, 39.81%, 50.49%, 59.12% and 69.59% were selected and noted as 30 vol.%, 40 vol.%, 50 vol.%, 60 vol.% and 70 vol.%-silk for mechanical property analysis. Volume fractions were calculated from the density values and mass fractions of the silk, epoxy and the final composite. The density of each composite specimen was measured by drainage method using an electronic density balance (FA1104J).

To minimize microstructural defects in the composites, a vacuum treatment (100 Pa for 1 h) prior to hot pressing was added to facilitate resin transfer and air bubble removal. Additionally, a comparison was made for the 60 vol.% silk reinforced composites with and without the vacuum treatment, which was labelled 60%(N).

2.3. Microstructural and morphological analyses

The morphology and microstructures of the plain weave silk fabric and the manufactured silk-epoxy resin composites were imaged on the surface and in cross sectional views using optical (OM, Shanghai Optical Instruments Co. Ltd., China) and scanning electron microscopy (SEM, JEOL JSM-6010, Japan). SEM images were taken at 20 kV accelerating voltage under secondary electron image mode.

2.4. Quasi-static mechanical testing

Uniaxial tensile mechanical properties were measured according to the Chinese Standard GB/T1040-92 test procedure on an Instron 8801 screw-driven testing machine (Instron Corp., Norwood, MA, USA), at a displacement rate of 2 mm min^{-1}. Corresponding flexural mechanical properties were measured according to the Chinese Standard GB/T1449-2005 test procedure on an Instron 5565 screw-driven testing machine, also at a displacement rate of 2 mm min^{-1}. Interlaminar shear tests were performed on the same machine at a displacement rate of 1 mm min^{-1}, according to International Standard ISO 14130:1997. All SFRPs were prepared using water-cutting to a dimensional accuracy of ±0.1 mm.

2.5. Impact testing

Impact mechanical testing was conducted according to International Standard ISO 179:1997 on a pendulum impact testing machine (MTS model ZBC 1000, MTS Corp., Eden Prairie, MN, USA). Unnotched specimens were loaded flat-wise with a 4 J hammer.

2.6. Dynamic mechanical thermal analysis

To examine the thermo-mechanical properties of the silk composites and the effect of the silk reinforcement volume fraction, dynamic mechanical thermal analysis (DMTA) was performed on a dynamic mechanical analyser (TA Instruments, Waters Ltd., DMA Q800) under cantilever mode at a fixed frequency of 1 Hz and a heating rate of 3 °C min^{-1} at temperatures from 25 to 170 °C. The dynamic strain was set at 0.2% for the cantilever mode. The dimensions of the test specimens were rectangular 25 mm × 10 mm × 2 mm.

3. Results and discussion

3.1. Morphology and microstructure of silk fabric and composites

The fibre alignment was found to have a significant influence on the compaction behaviour of the composites during processing [26,27]. Optical and scanning electron microscopy images of the structure of the silk fabric reinforcement and resultant SFRPs, presented in Fig. 1, show that the silk fabric was tightly woven with little porosity between the fibres with dozens of silk threads in orthogonal directions (Fig. 1a–c). The areal density of the silk fabric was measured to be 90 g m^{-2}, which imparts a high packing density in the composite. Shah et al. [1] argued that the irregular (almost-triangular) shape of single *B. mori* silk fibres with their concave and convex cross-sections could permit higher 'intra-yarn' packing densities than with irregular polygonal cross-sections of common plant fibres, which was also a reason that silk fabric had a more favourable compaction response than plant fibre textiles in the composite formation. However, as the reinforcement fractions of as high as 70 vol.% were achieved, specifically with hot pressing at moulding pressures up to 10 MPa, our study clearly validates these claims of the better compaction behaviour of the silk fabric.

Fig. 1d–f shows the cross-sectional microstructure and morphology of the manufactured silk composites, where it is clear that the resin was well infiltrated in between reinforcement silk fibres to form a continuous matrix. The concave and convex cross-sections of silk fibres,

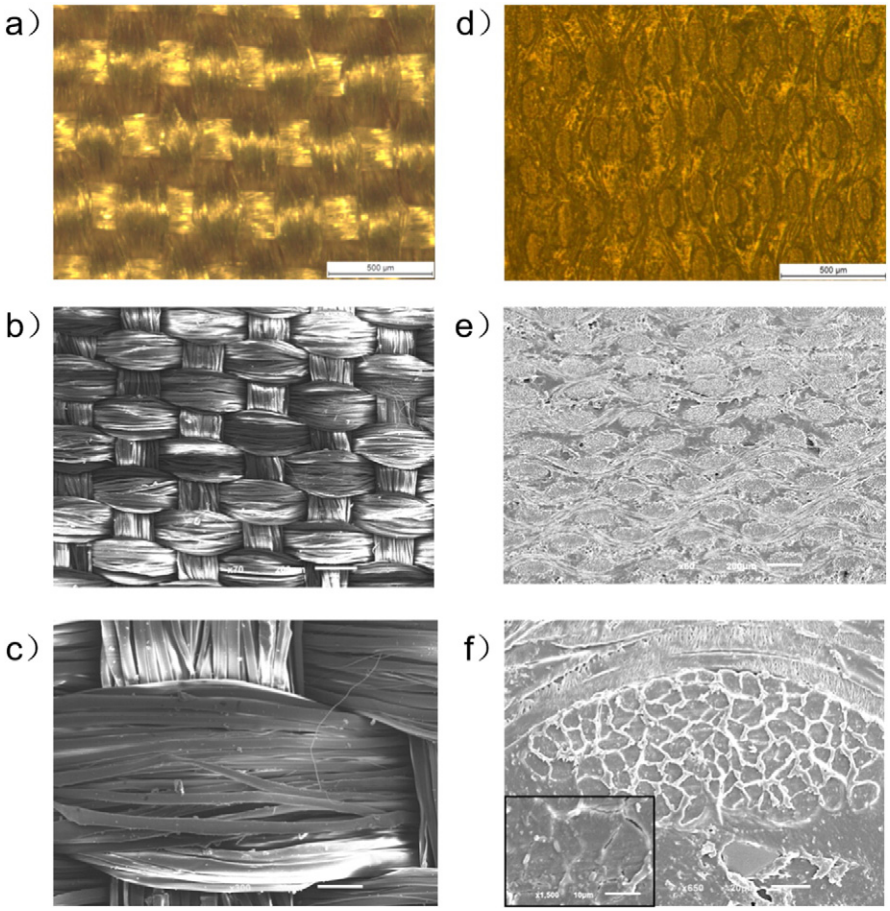

Fig. 1. Optical (OM) and scanning electron (SEM) microscopy images of the microstructure of the (a–c) silk fibre reinforcements and (d–f) the resulting SFRPs, showing: (a) surface OM, (b) surface SEM and (c) enlarged single yarn SEM image of the plain weave silk fabric; (d) cross-section OM, (e) cross-section SEM, and (f) enlarged single yarn cross-section SEM image of the SFRPs. Scale bars represent 500 μm in (a, b, d and e), 100 μm in (c and f) and 10 μm in inset (f).

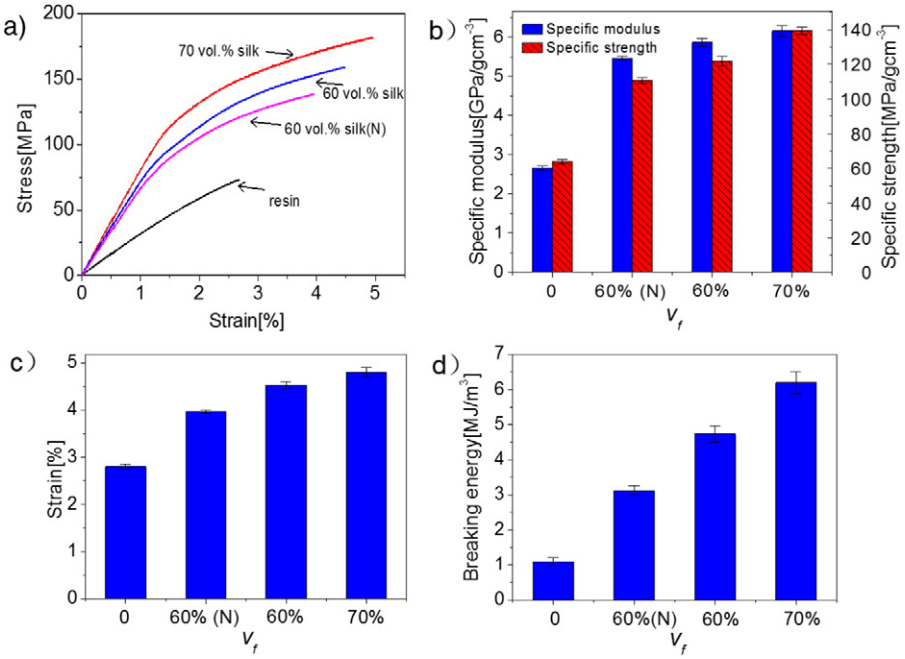

Fig. 2. Tensile properties of epoxy resin and SFRPs. (a) Tensile stress-strain curves of epoxy resin and SFRPs, 60 vol.%-silk, 70 vol.%-silk and 60 vol.%-silk(N) (without vacuum treatment); (b) specific modulus and specific strength of the epoxy resin and SFRPs; (c) ultimate strain of epoxy resin and SFRPs; (d) breaking energy of the epoxy resin and SFRPs. (b–d) are plotted as a function of the volume fraction v_f of silk reinforcement.

which are evident in Fig. 1f, can indeed be seen to enable close packing of fibres, but because of our manufacturing procedures the resin matrix still penetrates the gaps between the fibres despite their tight packing. Prior to curing, the viscosity of epoxy resin was measured to be low (~40 mPa s) and the relatively easy flow enabled good wetting of the silk fibre; during curing, a temperature of 120 °C and a holding time of 2 h were chosen to sufficiently cross-link the epoxy and to form fibre-matrix bonds without thermally degrading the protein fibres, which is critical [28]. For some composites, a vacuum treatment was applied before hot pressing, which was intended to reduce the presence of microstructural defects such as voids. Additionally, a rapid moulding-closing speed was used to avoid premature gelation, followed by an appropriate rate of cooling after the isothermal hot-press procedure to relieve the stresses from cross-linking reactions and the thermal treatment [29,30].

3.2. Quasi-static mechanical properties

3.2.1. Tensile properties

Typical uniaxial tensile stress-strain curves of pristine epoxy resin and SFRPs (60 vol.%-silk(N), 60 vol.%-silk and 70 vol.%-silk) are presented in Fig. 2. The key mechanical properties including modulus, ultimate strength and strain at the maximum stress and breaking energy derived from the stress-strain curves from the tensile, flexural and impact mechanical tests performed on at least three specimens for each volume fraction, are summarized in Table 2. Breaking energy is calculated as the area under the stress-strain curve and the unit is converted from MPa to MJ m^{-3} for easy comparison with the literature. The SFRPs exhibit enhanced tensile mechanical properties with a higher modulus and strength compared to pure epoxy resin. The highest tensile modulus and strength (E_t = 7.8 GPa, σ_t = 177 MPa) were found for the 70 vol.%-silk SRFP, which were more than double of that of pure epoxy resin. In particular, the breaking energy of 70 vol.%-silk SFRP increased by over 450% compared to that of pristine epoxy resin. Notably, with 10% increase in the volume fraction of silk from 60 vol.% to 70 vol.%, both the tensile strength (σ_t) and the strain at maximum stress (ε_t) increased further, resulting in a 30% improvement in the breaking energy.

To evaluate the effectiveness of the vacuum treatment in reducing defects in our manufacturing procedure, a comparison of 60 vol.% silk SFRPs was made with and without the treatment. Results in Fig. 2 and Table 2 show that the vacuum pre-treatment helped to improve the tensile properties of the composites, with the modulus and strength increased by ~8 and 10%, respectively. The effect is presumed to occur because the vacuum facilitates the resin transfer into the fibre gaps, propelling the air bubbles out, thereby enhancing the fibre-matrix interfacial bonding. The enhancement in the interfacial bonding through vacuum treatment can be seen more directly from the results of interlaminar shear experiment, as discussed later. It should be noted that this increase in modulus is less significant than the corresponding increase in strength; we believe that this follows because the modulus is derived from the initial low strain region where the fibre-matrix bonding strength does not play such an important role as for the larger strain region approaching failure.

SEM images of the fracture surface morphology of pure epoxy resin and 70 vol.%-silk SFRP are shown in Fig. 3. In contrast to the sharp cleavage features on the fracture surfaces for pristine epoxy resin, the composites contained fractured fibres and hole sites left from pulled-out fibres. Such evidence of fibre pull-out and fracture is indicative of good fibre-matrix interfacial bonding of the SFRPs, which contributes to the improved mechanical performance.

Based on the fracture mechanics of composites [31,32], in a brittle matrix-ductile fibre composite system, initially the stress is shared by the fibre and matrix; once the matrix resin fractures, the fibres act to confer apparent ductility, i.e., by acting as crack stoppers to delay catastrophic failure of the material, until fracture of the fibres occurs. In this regard, provided the fibre-matrix interaction is large enough, the tensile properties of the ductile reinforcement fibres can significantly enhance the toughness of the composites [5,33]. Based on numerous studies on silk fibres [3,34,35], it is known that silk fibres are more extensible and tougher than epoxy resin [36,37]; indeed, the breaking energy of *B. mori* silk fibres can be as much as four times of that of the epoxy resin. The high toughness of the silk fibre, attributed to its high density of hydrogen-bonding in its molecular structure, clearly shows potential to enhance the toughness of fibre-reinforced composites. Although the 70 vol.%-silk SFRP displays much higher toughness and fracture strain than the unreinforced matrix, there is still room for improvement considering that a better-matched epoxy resin matrix can be chosen. Nevertheless, compared with the previously studied flax and glass fibre composites [22,38,39], the tensile toughness properties of SFRPs measured in this study are much better, which could make SFRPs attractive for many structural engineering applications that are toughness-critical.

3.2.2. Flexural properties

Fig. 4a, b shows two groups of flexural stress–strain curves for the epoxy resin and SFRPs. In Fig. 4a, a comparison between pure epoxy resin and the 60 vol.%-silk SFRPs indicates that the average flexural modulus and flexural strength of the silk composites increased by ~200% and 144% for the vacuum-treated, and ~135% and 65% for the non-vacuum-treated. Notably, in the absence of the vacuum treatment, the properties of the silk composites showed a larger variability across specimens (Fig. 4c), which could be attributed to the uneven distribution of defects such as voids. Akin to the tensile mechanical properties of SFRPs (Fig. 3), it is apparent that large v_f of silk fabric reinforcements acts to significantly improve the flexural strength of the epoxy resin.

Table 2
Mechanical properties of the epoxy resin and SFRPs.
E_t: tensile modulus (GPa), ρ: density, E_t/ρ: specific tensile modulus (GPa/g cm^{-3}), σ_t: tensile strength (MPa), σ_t/ρ: specific tensile strength (MPa/g cm^{-3}), ε_t: ultimate tensile strain (%), BE_t: tensile fracture energy (MJ m^{-3}), E_f: flexural modulus (GPa), ρ: density, E_f/ρ: specific flexural modulus (GPa/g cm^{-3}), σ_f: flexural strength (MPa), σ_f/ρ: specific flexural strength (MPa/g cm^{-3}), ε_f: ultimate flexural strain (%), BE_f: flexural fracture energy (MJ m^{-3}), σ_i: impact strength (kJ m^{-2}), σ_i/ρ: specific impact strength (kJ m^{-2}/g cm^{-3}).

Specimen	Tensile properties						Flexural properties						Impact properties	
	E_t	E_t/ρ	σ_t	σ_t/ρ	ε_t	BE_t	E_f	E_f/ρ	σ_f	σ_f/ρ	ε_f	BE_f	σ_i	σ_i/ρ
Epoxy resin	3.2 ± 0.1	2.7 ± 0.1	76.6 ± 1.3	63.8 ± 1.1	2.8 ± 0.1	1.1 ± 0.1	3.5 ± 0.0	2.9 ± 0.0	134.2 ± 6.4	111.8 ± 5.3	3.9 ± 0.1	3.0 ± 0.2	12.8 ± 0.2	10.7 ± 0.1
30 vol.%-silk	–	–	–	–	–	–	5.6 ± 0.0	4.6 ± 0.0	209.8 ± 3.8	170.6 ± 3.1	4.6 ± 0.1	5.8 ± 0.2	18.5 ± 1.4	15.0 ± 1.2
40 vol.%-silk	–	–	–	–	–	–	7.5 ± 0.1	6.1 ± 0.1	215.0 ± 3.9	173.4 ± 3.2	3.5 ± 0.0	4.1 ± 0.3	18.6 ± 0.1	15.0 ± 0.1
50 vol.%-silk	–	–	–	–	–	–	8.9 ± 0.1	7.1 ± 0.1	249.3 ± 3.1	199.4 ± 2.5	3.7 ± 0.0	5.5 ± 0.2	22.8 ± 0.1	18.3 ± 0.1
60 vol.%-silk(N)	6.9 ± 0.1	5.5 ± 0.1	139.3 ± 2.1	110.6 ± 1.7	4.0 ± 0.0	3.1 ± 0.1	8.1 ± 0.7	6.4 ± 0.5	232.3 ± 18.0	184.4 ± 14.3	3.6 ± 0.1	5.9 ± 0.6	57.3 ± 5.7	45.4 ± 4.5
60 vol.%-silk	7.4 ± 0.1	5.9 ± 0.1	153.5 ± 3.7	121.8 ± 3.0	4.5 ± 0.1	4.7 ± 0.2	10.5 ± 0.1	8.3 ± 0.1	343.8 ± 5.1	272.9 ± 4.1	4.5 ± 0.1	9.2 ± 0.4	70.7 ± 1.7	56.1 ± 1.4
70 vol.%-silk	7.8 ± 0.2	6.2 ± 0.1	176.9 ± 2.6	139.2 ± 2.1	4.8 ± 0.1	6.2 ± 0.3	12.5 ± 0.1	9.8 ± 0.1	337.5 ± 11.4	265.7 ± 9.0	3.8 ± 0.0	7.2 ± 0.6	60.0 ± 3.2	47.2 ± 2.5

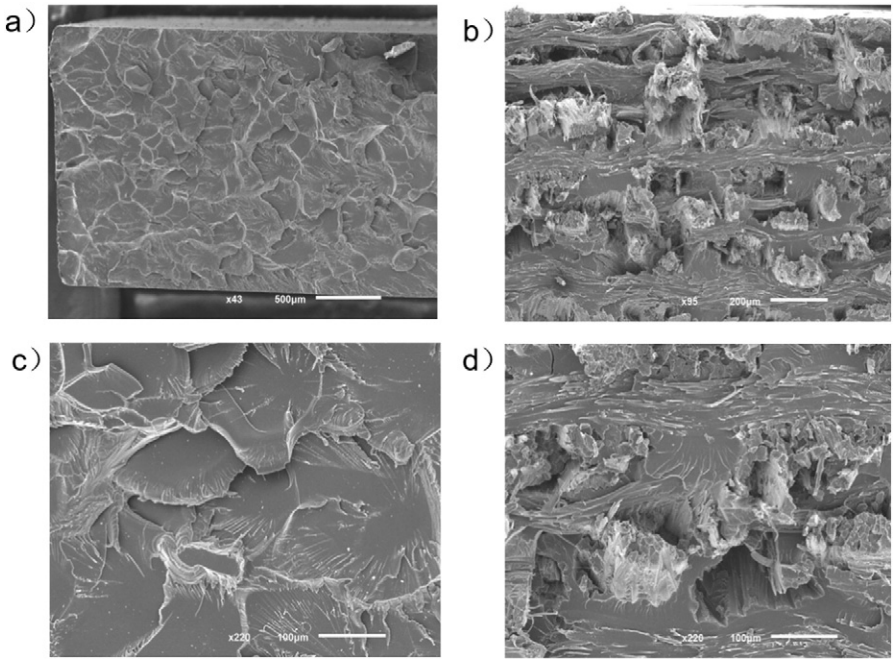

Fig. 3. SEM images of the tensile fracture surface of (a), (c) epoxy resin and (b), (d) 70 vol.%-silk SFRP.

The effect of the volume fraction v_f of silk reinforcements on the flexural mechanical properties of SFRPs is evaluated in detail in Fig. 4b and Table 2. With increasing v_f, the flexural modulus and strength of the composite increased, respectively, from 5.6 GPa and 210 MPa for 30 vol.%-silk to 12.5 GPa and 337 MPa for 70 vol.%-silk. The flexural modulus and strength increased almost linearly with increasing silk volume fraction from 30% to 60%. The fitted lines had correlation coefficient R^2 of 0.96 for the modulus and 0.83 for the strength. However, as the v_f of silk increased from 60% to 70%, the flexural strength and specific strength were essentially unchanged, which suggest that the v_f for optimal flexural strength is 60 vol.%. Such mechanical properties are comparable to the plain woven glass fibre reinforced epoxy composites [22], which is a notable achievement as the epoxy matrix was not specifically selected for its mechanical properties but rather for its low cost. Additionally, the ultimate strain was slightly less than the pristine epoxy resin for all SFRPs except with 30 vol.%-silk and 60 vol.%-silk. The constant ultimate strain for most SFRPs in flexure tests suggests that the silk reinforcements could not change the essential brittleness or failure mode of the epoxy matrix in flexure mode, despite their significant contributions to the strength and stiffness of the composites. During flexural testing, the specimen was subject to a complex mode of deformations including tensile, compressive, bending and shear loading depending on

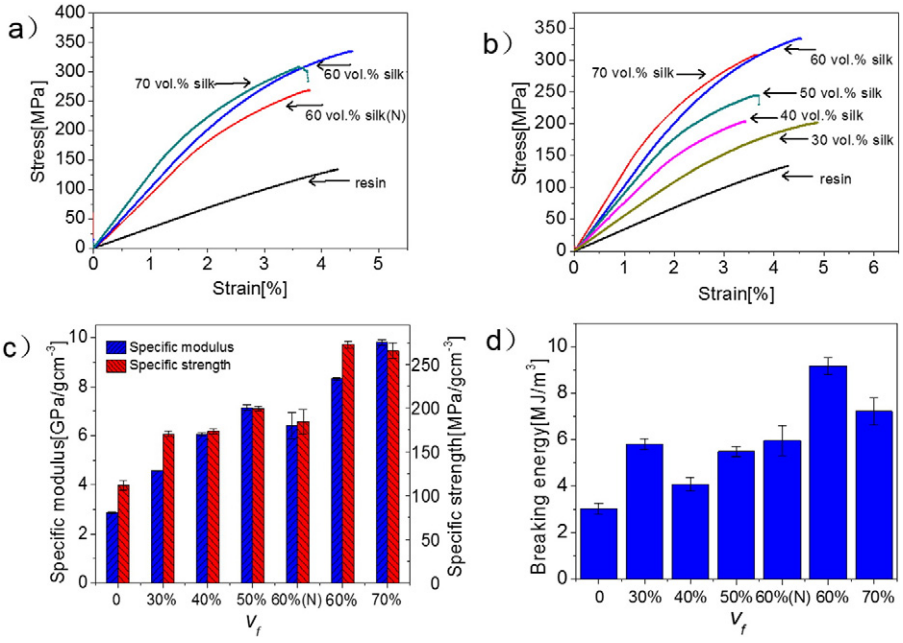

Fig. 4. Flexural properties of epoxy resin and SFRPs. (a) Flexural stress-strain curves of epoxy resin and SFRPs (60 vol.%-silk, 60 vol.%-silk(N), 70 vol.%-silk) for the effect of vacuum treatment; (b) flexural stress-strain curves of epoxy resin and SFRPs (30 vol.%-silk, 40 vol.%-silk, 50 vol.%-silk, 60 vol.%-silk and 70 vol.%-silk) for the effect of fibre volume fraction v_f; (c) specific flexural modulus and specific flexural strength of the epoxy resin and SFRPs; (d) breaking energy of the epoxy resin and SFRPs.

the position of the specimen [40]. The only marginal improvement in the strain capacity of the composites, compared to that of the pure epoxy, under such flexural loading suggests that the silk fibre-epoxy interface properties may need to be further optimized to achieve the best combination of stiffness, strength and ductility in these materials. Shah et al. [4] reported a higher ultimate strain of, respectively, 6.9% and 5.2% under flexural and tensile loading for a woven silk-epoxy composite prepared by vacuum-driven resin transfer; these are higher than our reported values. Apparently, vacuum-driven resin transfer methods could be more effective in infusing epoxy to the reinforcement silk and improving interfacial bonding. Additionally, an epoxy resin system that had a much higher tensile failure strain (ε_f ~ 12–16%) was used in Shah's study, as compared to the more brittle epoxy system (where ε_f ~ 3%) used here. Clearly, through tuning of the fabrication technique and a careful selection of the matrix resin system, we could potentially achieve further increases in flexural properties for the SFRPs.

3.2.3. Interlaminar shear properties

The interlaminar shear strength (ILSS) test directly evaluates the interfacial properties between the fibre reinforcements and the matrix in the composite. Fig. 5 and Table 2 show that the ILSS of the 60 vol.% SFRP (34 MPa) could be as much as 240% higher than that of plain woven flax fibre epoxy composites representing plant fibre reinforced plastics (PFRPs) [22,39,41], but lower than that of plain woven glass fibre epoxy composites (GFRPs) [22,41]. In this test, it could be concluded that vacuum treatment was critical to enhance the interfacial properties of SRFPs. It resulted in an increase of ~47% in the average ILSS for 60 vol.%-silk compared to 60 vol.%-silk(N).

The good interfacial properties of SFRPs could be explained by two features. Chemically, *B. mori* silk fibres contain both hydrophobic and hydrophilic structural domains [42], which allow both polar-polar and hydrophobic interactions with the chemical groups in the epoxy matrix. However, morphologically, the strong interfacial interactions may be compromised by a disadvantageous contribution from the smooth surface morphology of silk fibres compared to flax fibres with rougher surfaces, as suggested in other studies [41]. It is believed that in our case the stronger interfacial group interactions dominate and result in the observed better interfacial properties for SFRPs.

3.2.4. Impact properties

As the aim of this work was to manufacture a tough composite from a brittle epoxy material, the impact strength (IS) and specific impact strength (SIS), to certain extent, become the most important measures in this work. From Table 2 and Fig. 6, it is apparent that the effect of silk reinforcements in improving the impact resistance of SRFPs only becomes prominent for silk-fibre volume fractions above 60%, where the impact strength surges to 71 kJ m^{-2}. Below 60 vol.%, there is only a mild effect of the silk-reinforcement, in contrast to the linear increasing trend for flexural properties (Fig. 4). It is again worth mentioning that in this work SFRPs were manufactured with the highest volume fractions of silk reinforcements to date (v_f = 60% and 70%). With such high fibre volume fraction, we effectively ensured that the fibres carried at least 10 times the load that was carried by the matrix, according to classical fibre-composite mechanics [1]. In addition to the greater load-carrying capacity of silk reinforcements, this high fraction of silk fibres serves to inhibit crack advance and induce significant deflection of the crack path, both of which are potent crack propagation toughening mechanisms.

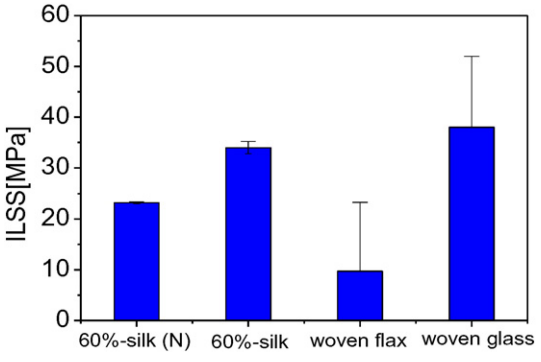

Fig. 5. Interlaminar shear strength (ILSS) (unit: MPa) of SFRPs (60 vol.%-silk and 60 vol.%-silk(N)) compared with flax and glass fibre plain woven epoxy composites.

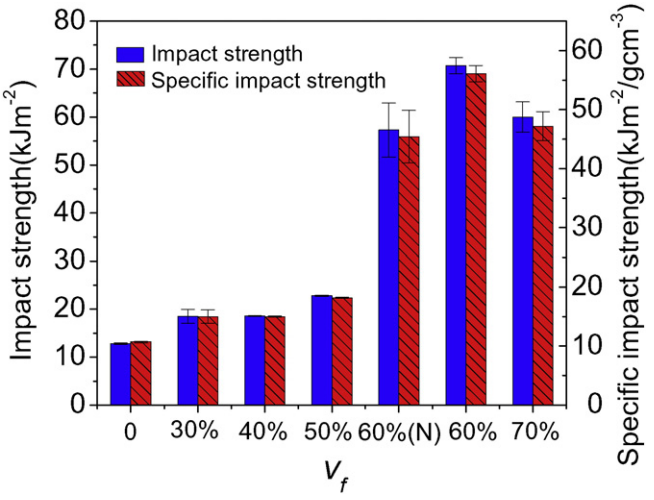

Fig. 6. Impact properties of different fibre volume fractions v_f of SFRPs: impact strength (kJ m^{-2}) and specific impact strength (kJ m^{-2}/g cm^{-3}).

3.3. Dynamic mechanical thermal analysis (DMTA)

Dynamic mechanical thermal analysis (DMTA) is conventionally used to study the mechanical properties and viscoelastic behaviour of polymers and polymer-based materials such as epoxy composites as a function of temperature, frequency and time [43,44]. DMTA experiments were conducted here for two purposes: firstly, the thermo-mechanical properties of the composite could be obtained, which are key properties for future engineering applications (especially those temperature-dependent); and secondly, it is expected to reveal the relaxation mechanisms of the constituent silk fibre and epoxy matrix at the molecular level.

Fig. 7a, c shows the changes of the storage modulus E' and tanδ (as a ratio of loss modulus E'' over storage modulus E') of the pristine epoxy resin and SFRPs with different volume fractions over a temperature range of 25–170 °C. Fig. 7b further compares the storage moduli of these specimens of different v_f at room temperature (prior to the glass transition) and at 140 °C (after the glass transition). Clearly the SFRPs with higher volume fractions possessed higher E', and E' also appeared in linear relationship with v_f. For example, at 25 °C E' for the 70 vol.%-silk SFRPs is 7250 MPa, which is roughly double that for the 30 vol.% silk SFRPs. More importantly, the storage modulus at 140 °C for the 50 vol.% and 60 vol.%-silk SFRPs is higher than 1000 MPa, compared to a reduction factor of 100 for epoxy through its glass-transition temperature T_g. In Fig. 7c, the pristine epoxy displayed a main tanδ peak at 115 °C, which corresponds to its T_g, and a minor peak at about 100 °C. Native *B. mori* silk's T_g is 220 °C [45], which is significantly higher than that of pristine epoxy. However, simply embedding silks in epoxy does not appear to alter the T_g of the matrix epoxy. As the content of silk increased in SFRPs, the peak tanδ values decreased in linear proportion to the reduced epoxy content, as shown in Fig.7d. One use of this relationship may be linking the volume fraction of the reinforcement fibre to the mechanical loss behaviours of SFRPs. This significant enhancement in the modulus of SFRPs for the studied temperature range, especially for

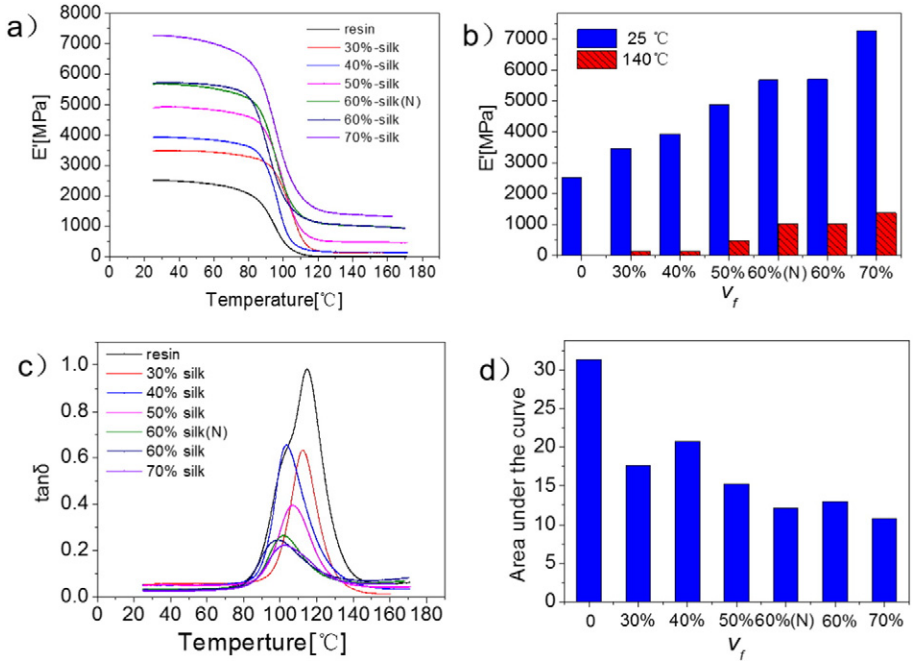

Fig. 7. Dynamic mechanical property profiles of epoxy resin and SFRPs in single cantilever mode (a) storage modulus E' and (c) loss tangent tanδ as a function of temperature from 25 °C to 170 °C; and (b) E' at two temperatures and (d) accumulated tanδ as function of volume fraction v_f of silk reinforcement.

temperatures above T_g (115 °C for epoxy resin), could certainly extend the use of these epoxy composites to a wider temperature range.

The bulk mechanical properties of a polymer at any given temperature are dependent on: i) the ability to elastically store mechanical energy corresponding to the measured elastic storage modulus E' in DMTA, and ii) the ability to dissipate mechanical energy through structural relaxations corresponding to the measured loss modulus E'' in DMTA. The peaks of the loss factor tan δ as the ratio of E''/E' directly indicate molecular relaxation events, i.e., a peak at about −60 °C for hydrocarbon polymers denoting the activation of motions in hydrocarbon side groups. In order to reveal the underlying mechanisms of the measured mechanical properties at room temperature, low temperature DMTA experiment from −150 °C to 25 °C was conducted. The results shown in Fig. 8 suggest that: i) the elastic storage modulus for the 60 vol.%-silk composite is much higher than the 30 vol.%-silk composite and the resin; and ii) both pristine resin and the composites with silk reinforcements possess low temperature structural relaxation events. Although the molecular relaxation mechanisms are different between epoxy and silk (β-relaxation for epoxy and silk-water complex's glass transition for silk), the structural relaxations below room temperature have similar effect for both epoxy and silk as the magnitude of tanδ is very close. Therefore, the modulus difference appears to be the main reason for the property enhancement in the tensile and flexure mechanical tests after introducing silk reinforcement. This is in line with the observations presented in this study. For example, the flexural modulus was increased with increasing silk content; however, the failure strain related to the plasticity or the dissipation ability of molecular structures did not change. Nevertheless, it remains unexplained why the high-v_f silk composites have disproportionally high impact strength. Further experiments with respect to molecular relaxations in SFRPs at impact rates are required and will be followed up in our future work.

4. Conclusions

In this work, a series of silk fabric reinforced epoxy composites (SFRPs) has been successfully manufactured using simple hand lay-up and hot-pressing techniques. Volume fractions of the silk fabric reinforcements in these SFRPs were varied from 30 vol.% to a value of 70 vol.%, which is the highest degree of silk-reinforcement for a silk-epoxy composite to date. The focus of this study was to examine the tensile mechanical properties, flexural mechanical properties and impact performance, as well as whether the silk reinforcement can improve the performance of brittle epoxy matrix. Results show that for 70 vol.%-silk SFRP, the tensile Young's modulus, ultimate stress and

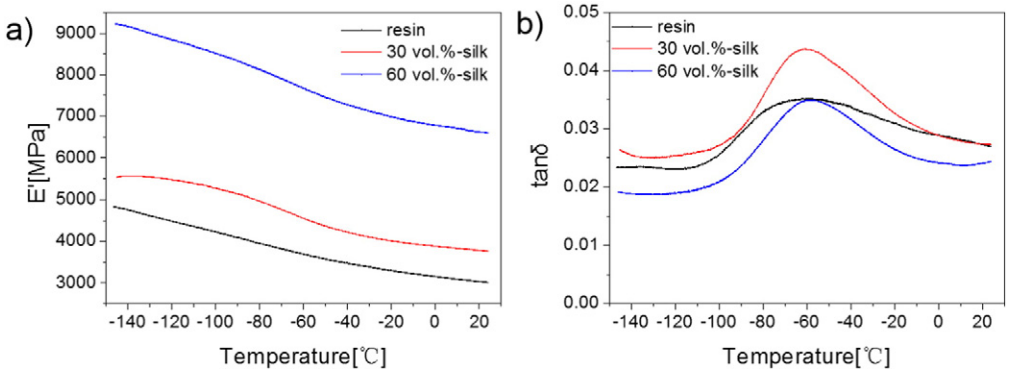

Fig. 8. Low temperature dynamic mechanical property profiles from −150 °C to 25 °C for epoxy resin, 30 vol.% and 60 vol.% SFRPs in single cantilever mode: (a) storage modulus E' and (b) loss tangent tanδ.

ultimate strain are all increased significantly, respectively, by 145%, 130% and 70%. Although the flexural Young's modulus and ultimate stress both increased, the strain capacity under the flexural mode was essentially unchanged with respect to that of the unreinforced epoxy matrix. The impact strength was also increased by silk-reinforcements, but only significantly for volume fractions above 60%. Dynamic mechanical thermal analysis further showed that the current SFRPs with high silk fibre volume fractions possess a high dynamic storage modulus, which exceeded 1000 MPa at 140 °C, and a low loss factor, with $\tan\delta < 0.2$, through the glass transition of the epoxy matrix. We believe that our findings will enrich the database of natural fibre-reinforced plastics as well as shed light on improving the weak and brittle performance of commercial epoxy resin through incorporating tough and strong silks as reinforcements.

Acknowledgments

This study was supported by funding from the National Natural Science Foundation of China [51503009], the State Key Laboratory of Molecular Engineering of Polymer (Fudan University) [K2016-05], and Beihang University. ROR acknowledges support from U.S. Department of Energy, Office of Science, Office of Basic Energy Sciences, Materials Sciences and Engineering Division, under contract no. DE-AC02-05CH11231.

We also thank Prof. Fritz Vollrath for his helpful comments and discussion on the subject of silk reinforced polymer resins.

References

[1] D.U. Shah, D. Porter, F. Vollrath, Opportunities for silk textiles in reinforced biocomposites: studying through-thickness compaction behaviour, Compos. A: Appl. Sci. Manuf. 62 (2014) 1–10.
[2] O. Faruk, A.K. Bledzki, H. Fink, M. Sain, Biocomposites reinforced with natural fibers: 2000–2010, Prog. Polym. Sci. 37 (2012) 1552–1596.
[3] Z.Z. Shao, F. Vollrath, Materials: surprising strength of silkworm silk, Nature 418 (2002) 741.
[4] D.U. Shah, D. Porter, F. Vollrath, Can silk become an effective reinforcing fibre? A property comparison with flax and glass reinforced composites, Compos. Sci. Technol. 101 (2014) 173–183.
[5] M. Ho, K. Lau, H. Wang, D. Bhattacharyya, Characteristics of a silk fibre reinforced biodegradable plastic, Compos. Part B 42 (2011) 117–122.
[6] Y. Zhao, H. Cheung, K. Lau, C. Xu, D. Zhao, H. Li, Silkworm silk/poly(lactic acid) biocomposites: dynamic mechanical, thermal and biodegradable properties, Polym. Degrad. Stab. 95 (2010) 1978–1987.
[7] Q.T.H. Shubhra, A.K.M.M. Alam, M.D.H. Beg, Mechanical and degradation characteristics of natural silk fiber reinforced gelatin composites, Mater. Lett. 65 (2011) 333–336.
[8] W. Li, X. Qiao, K. Sun, X. Chen, Mechanical and viscoelastic properties of novel silk fibroin fiber/poly(epsilon-caprolactone) biocomposites, J. Appl. Polym. Sci. 110 (2008) 134–139.
[9] Q. Yuan, J. Yao, X. Chen, L. Huang, Z. Shao, The preparation of high performance silk fiber/fibroin composite, Polymer 51 (2010) 4843–4849.
[10] Y. Wang, B. Zhang, J. Ye, Microstructures and toughening mechanisms of organoclay/polyethersulphone/epoxy hybrid nanocomposites, Mater. Sci. Eng. A 528 (2011) 7999–8005.
[11] R. Thomas, D. Yumei, H. Yuelong, Y. Le, P. Moldenaers, Y. Weimin, et al., Miscibility, morphology, thermal, and mechanical properties of a DGEBA based epoxy resin toughened with a liquid rubber, Polymer 49 (2008) 278–294.
[12] P. Jain, V. Choudhary, I.K. Varma, Effect of structure on thermal behaviour of epoxy resins, Eur. Polym. J. 39 (2003) 181–187.
[13] K. Mimura, H. Ito, Characteristics of epoxy resin cured with in situ polymerized curing agent, Polymer 43 (2002) 7559–7566.
[14] X. Zhang, Y. Min, Z. Hua, Epoxy-based electronic materials containing nitrogen heterocyclic ring: flame retardancy, Prog. Chem. 26 (2014) 1021–1031.
[15] H. Zhou, S. Zhao, W. Yu, H. Jiang, C. Guo, Y. Li, Research on performance of flame-retardant epoxy resin electronic packaging materials, in: B. Xu, H.Y. Li (Eds.),Advanced Materials Research 2013, pp. 117–120.
[16] A. Toldy, B. Szolnoki, G. Marosi, Flame retardancy of fibre-reinforced epoxy resin composites for aerospace applications, Polym. Degrad. Stab. 96 (2011) 371–376.
[17] Y. Shih, Mechanical and thermal properties of waste water bamboo husk fiber reinforced epoxy composites, Mater. Sci. Eng. A 445–446 (2007) 289–295.
[18] M. Di Filippo, S. Alessi, G. Pitarresi, M.A. Sabatino, A. Zucchelli, C. Dispenza, Hydrothermal aging of carbon reinforced epoxy laminates with nanofibrous mats as toughening interlayers, Polym. Degrad. Stab. 126 (2016) 188–195.
[19] A. Chira, A. Kumar, T. Vlach, L. Laiblová, A.S. Škapin, P. Hájek, Property improvements of alkali resistant glass fibres/epoxy composite with nanosilica for textile reinforced concrete applications, Mater. Des. 89 (2016) 146–155.
[20] J. Lu, J.P. Youngblood, Adhesive bonding of carbon fiber reinforced composite using UV-curing epoxy resin, Compos. Part B 82 (2015) 221–225.
[21] H. Ibrahim, M. Farag, H. Megahed, S. Mehanny, Characteristics of starch-based biodegradable composites reinforced with date palm and flax fibers, Carbohydr. Polym. 101 (2014) 11–19.
[22] D.U. Shah, Natural fibre composites: comprehensive Ashby-type materials selection charts, Mater. Des. 62 (2014) 21–31.
[23] M. Jawaid, H.P.S. Abdul Khalil, B.A. Abu, Mechanical performance of oil palm empty fruit bunches/jute fibres reinforced epoxy hybrid composites, Mater. Sci. Eng. A 527 (2010) 7944–7949.
[24] Q. Liu, M. Hughes, The fracture behaviour and toughness of woven flax fibre reinforced epoxy composites, Compos. A: Appl. Sci. Manuf. 39 (2008) 1644–1652.
[25] K. Bunko, J.F. Kennedy, Handbook of Fiber Chemistry, third ed.69 CRC Press LLC, 2007 612.
[26] D.U. Shah, P.J. Schubel, M.J. Clifford, Modelling the effect of yarn twist on the tensile strength of unidirectional plant fibre yarn composites, J. Compos. Mater. 47 (2013) 425–436.
[27] Y.R. Kim, S.P. McCarthy, J.P. Fanucci, Compressibility and relaxation of fiber reinforcements during composite processing, Polym. Compos. 12 (1991) 13–19.
[28] M. Ho, H. Wang, J. Lee, C. Ho, K. Lau, J. Leng, et al., Critical factors on manufacturing processes of natural fibre composites, Compos. Part B 43 (2012) 3549–3562.
[29] PK M, Fiber-reinforced Composites Materials, Manufacturing, and Design, CRC Press, 2007.
[30] K.T. Kim, J.H. Jeong, Y.T. Im, Effect of molding parameters on compression molded sheet molding compounds parts, J. Mater. Process. Technol. 67 (1997) 105–111.
[31] R. Brighenti, A. Carpinteri, D. Scorza, Fracture mechanics approach for a partially debonded cylindrical fibre, Compos. Part B 53 (2013) 169–178.
[32] L.S. Sigl, A.G. Evans, Effects of residual stress and frictional sliding on cracking and pull-out in brittle matrix composites, Mech. Mater. 8 (1989) 1–12.
[33] A.G. Facca, M.T. Kortschot, N. Yan, Predicting the tensile strength of natural fibre reinforced thermoplastics, Compos. Sci. Technol. 67 (2007) 2454–2466.
[34] P. Jiang, H.F. Liu, C.H. Wang, L.Z. Wu, J.G. Huang, C. Guo, Tensile behavior and morphology of differently degummed silkworm (*Bombyx mori*) cocoon silk fibres, Mater. Lett. 60 (2006) 919–925.
[35] J. Perez-Rigueiro, M. Elices, J. Llorca, C. Viney, Tensile properties of silkworm silk obtained by forced silking, J. Appl. Polym. Sci. 82 (2001) 1928–1935.
[36] E.H. Andrews, A. Stevenson, Fracture energy of epoxy resin under plane strain conditions, J. Mater. Sci. 13 (1978) 1680–1688.
[37] R. Griffiths, D.G. Holloway, The fracture energy of some epoxy resin materials, J. Mater. Sci. 5 (1970) 302–307.
[38] K. Adekunle, S. Cho, C. Patzelt, T. Blomfeldt, M. Skrifvars, Impact and flexural properties of flax fabrics and Lyocell fiber-reinforced bio-based thermoset, J. Reinf. Plast. Compos. 30 (2011) 685–697.
[39] S. Goutianos, T. Peijs, B. Nystrom, M. Skrifvars, Development of flax fibre based textile reinforcements for composite applications, Appl. Compos. Mater. 13 (2006) 199–215.
[40] C. Chamis, Test Methods and Design Allowables for Fibrous Composites, ASTM, 1989.
[41] D.U. Shah, Developing plant fibre composites for structural applications by optimising composite parameters: a critical review, J. Mater. Sci. 48 (2013) 6083–6107.
[42] F. Chen, X. Liu, H. Yang, B. Dong, Y. Zhou, D. Chen, et al., A simple one-step approach to fabrication of highly hydrophobic silk fabrics, Appl. Surf. Sci. 360 (2016) 207–212.
[43] S. Zainuddin, A. Fahim, T. Arifin, M.V. Hosur, M.M. Rahman, J.D. Tyson, et al., Optimization of mechanical and thermo-mechanical properties of epoxy and E-glass/epoxy composites using NH_2-MWCNTs, acetone solvent and combined dispersion methods, Compos. Struct. 110 (2014) 39–50.
[44] W.K. Goertzen, M.R. Kessler, Dynamic mechanical analysis of carbon/epoxy composites for structural pipeline repair, Compos. Part B 38 (2007) 1–9.
[45] G. Juan, P. David, V. Fritz, Thermally induced changes in dynamic mechanical properties of native silks, Biomacromolecules 14 (2013) 930–937.